Journal of
Nanoscience and Nanotechnology
Vol. 11, 3669–3679, 2011

Synthesis of Silver Nanoparticles by Oleylamine-Oleic Acid Reduction and Its Use in Making Nanocable by Coaxial Electrospinning

Simge Çınar[1], Güngör Gündüz[1,*], Bora Mavis[2], and Üner Çolak[3]

[1]*Kimya Mühendisliği Bölümü, Orta Doğu Teknik Üniversitesi, Ankara 06531, Turkey*
[2]*Makina Mühendisliği Bölümü, Hacettepe Üniversitesi, Beytepe, Ankara 06800, Turkey*
[3]*Nükleer Mühendislik Bölümü, Hacettepe Üniversitesi, Beytepe, Ankara 06800, Turkey*

In the present study, silver nanoparticles were produced by hydrazine hydrate and oleylamine/oleic acid systems in order to investigate the effects of reducing agents with different strengths on the reduction mechanism. Particle size and size distribution of silver particles produced by slow reducing system were studied in detail by using transmission electron microscopy (TEM), X-Ray Diffraction (XRD), photon correlation spectroscopy (PCS), and surface plasmon resonance spectroscopy (SPR). Finally, reduction mechanism by oleylamine and oleic acid system was clarified and particles with average diameter of 2.7 nm were produced. Nano-sized particles were then placed at the center of the polymer fibers by coaxial electrospinning and nanocable like structures were produced. SEM and TEM were used for the characterization of these cables.

Keywords: Electrospinning, Metal/Polymer Nanocomposite, Nanocable, Metal Nanoparticle, Silver, Oleylamine, Oleic Acid, Hydrazine Hydrate.

RESEARCH ARTICLE

1. INTRODUCTION

The control of size and shape of nanocomposites makes possible to make products with tunable properties. For metal–polymer composites, to control the size and shape of the metallic features in nano-scale makes them useful in applications like electronics, photonics, sensing, and memory circuits. Nanowires, for instance, are one dimensional nanostructures with their superior property of quantum confinement which does not normally exist in 3D structures.

Certain arrangement of particles in the nanowire structures is achieved by the methods of self assembly or ligand control; however, lengths of the nanowires produced by these methods are limited to a few micrometers with diameters of between 1 and 100 nm and aspect ratio of greater than twenty.[1] Nanocables, on the other hand, are one dimensional core–shell structures with longer lengths. If nanoparticles are placed axially at the center of the structures, metal core–polymer shell nanocables will be formed (Fig. 1).

It is difficult to make cable structures by simple electrospinning technique, because, metal particles may adversely affect the viscosity, which, in turn affects the Taylor cone where fiber jet originates out. An important point is that the amount of metal nanoparticles should be above a threshold value so-called percolation value so that metal nanoparticles embedded in polymer matrix touch each other in a continuous manner to conduct electrical current. Coaxial electrospinning can solve the problems faced in simple electrospinning.

In the literature, studies about the metal–polymer nanocable synthesis are very limited. In the study of Song et al. oleylamine capped iron–platinum particles were aligned in the core of polycaprolactone (PCL), and nanofibers with a length of approximately 3000 nm were obtained by coaxial electrospinning.[2] They produced the iron–platinum particles first, and then, used the solution containing these particles as a core solution in the electrospinning process. They used PCL to make the shell polymer, and its solution in trifluoroethanol (TFE) which is a strong solvent with high polarity was used in coaxial electrospinning.

In the present study, we have succeeded to make nanocable by coaxial electrospinning with silver as the nanowire inside PCL shell (Fig. 2). The production of silver nanoparticles will be discussed first, and then the production of nanocable by coaxial electrospinning will be investigated.

*Author to whom correspondence should be addressed.

 1533-4880/2011/11/3669/011 doi:10.1166/jnn.2011.3812

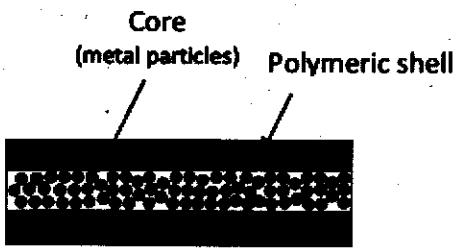

Fig. 1. Nanocable structure.

Silver is one of the most widely used metals in the form of nanoparticles due to its chemical inertness, low cost, and high electrical conductivity. Silver nitrate is the most widely used silver salt to produce ionic silver which can then be reduced.[3] In the present study, chemical reduction method was used to produce silver nanoparticle. The main objective is to obtain monodispersed particles with controlled sizes. In the chemical reduction method, this aim can be achieved by proper selection of reducing and capping agents. In this study, the importance of reducing agent and reduction mechanism were investigated in detail by comparing the effects of strong and weak agents on the reduction of silver nitrate.

Hydrazine is one of the strongest reducing agents for silver ions and it results in the production of large particles with uncontrolled size distribution.[4,5] To reduce the strong reduction action, reversed wormlike micelle with polymer shield system was suggested in this study. Ethanol addition to the system was also proposed in order to control particle growth. Thus, core–polymer shell structures could be formed by assemblies of reverse wormlike structures during electrospinning.

Oleylamine and oleic acid are used separately or together in many different systems. Since amine and carboxyl groups of oleylamine and oleic acid have weak reducing effect, they act as a reducer in the absence of any other stronger agent. On the other hand, their aliphatic tails and functional groups make them strong capping agents. However, when oleylamine or oleic acid is used alone in the system, reduction takes a long time or requires high temperatures to obtain monodispersed particles.

The study of Xu et al. was an example of systems in which oleylamine was used both as reducing agent and stabilizer. They synthesized ferrous oxide (FeO) particles by using oleic acid and oleylamine, at varying sizes between 14–100 nm which could be controlled by heating conditions. In their study, oleylamine was selected as alternative reducing agent and its excess amount enhanced the reduction reaction.[6] The same group also published their study on the reduction of ferric oxide (Fe_3O_4) by only oleylamine.[7] In this case, particles with diameter of 7–10 nm were produced after one hour aging at 300 °C.

Another example about the multifunctional effect of oleylamine was the study of Mazumder et al.[8] They concluded that oleylamine could be used as a solvent, surfactant, and reducing agent for reducing palladium ions. However, it cannot be used alone to synthesize monodisperse particles. This is due to longer reduction process leading to multi-nucleation and heterogeneous growth of nuclei. They have also added borane tributylamine complex to the system as co-reductant which is stronger than oleylamine.

According to these studies, it can be concluded that oleylamine has reducing effect on metal particles. However, it is so weak that either broad particle size distribution is obtained or high temperatures are needed. Otherwise, it should be used with another reducing agent which is stronger than oleylamine.

Oleic acid is a good companion for oleylamine due to their chemical similarity. There are several studies in the literature where oleylamine and oleic acid were used together for the stabilization and/or reduction of metal ions.[9–12] However, to our knowledge, none of the studies explain the mechanism of the reduction and effects of the oleylamine and oleic acid in the system completely. In

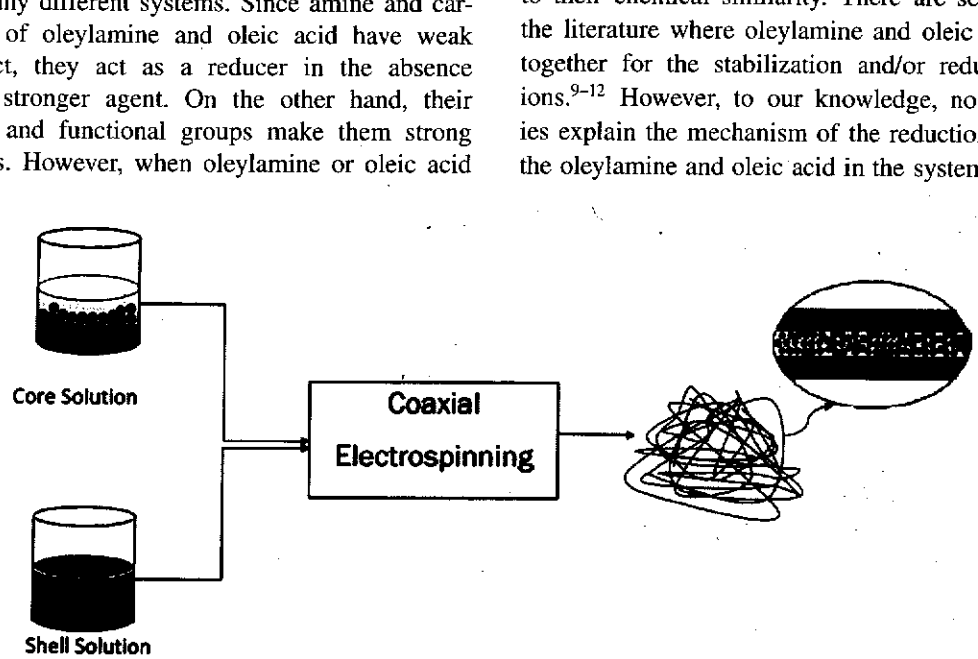

Fig. 2. Silver nanocable production.

RESEARCH ARTICLE

this study, their effects were also studied in detail and the mechanism was clarified.

2. EXPERIMENTAL DETAILS

Two separate systems were prepared to reduce silver nitrate to silver metal nanoparticles. In the first system, a strong reducing agent, hydrazine hydrate, was used. The prepared solution was directly electrospun with the aim of obtaining interconnected assemblies of metal particles inside fibers. In the second case, a weak reducing agent, oleylamine/oleic acid system, was used. In this system, metal particles were first produced, and then they were electrospun coaxially with a polymer to shield the particles at the center of fibers to obtain nanocables.

2.1. Hydrazine Hydrate System

In the system polyvinyl alcohol (PVA, Clarient, molecular weight: 23000), Dioctyl sulfosuccinate sodium salt (DSS, Sigma Aldrich, 98% purity), and deionized water (DIW, 18.2 MΩ) were used as shielding polymer, surfactant, and solvent, respectively. Initially silver nitrate (Merck, extra pure) solution was prepared in DIW. Then, DSS and PVA were added and the temperature was increased to 50 °C to dissolve the polymer. After 4 hours of mixing, a homogeneous solution was obtained, and hydrazine hydrate solution was added to the solution at room temperature. Hydrazine hydrate was diluted with ethanol and water to control its addition rate. Ethanol (Sigma Aldrich, ≥99.8) in the system serves as co-solvent and eliminates precipitation and oxidation of silver atoms, and slows down the reduction reaction.

The electrospinning setup consists of a high voltage direct current supply (GAMMA High Voltage Research Inc., USA, Model no: ES30P-20W/DAM, electrical potential range: 0–30 kV), a syringe pump (New Era Pump Systems Inc., model no: NE-1600 six-syringe pump) and a collector.

The positive electrode wire was attached to the metal body of the needle, whereas the negative pole was connected to the metal collector. The metal collector was covered by aluminum foil and the setup was kept in a poly(methyl methacrylate) cage for safety. The experiments were carried out at atmospheric pressure and at room temperature.

In the electrospinning experiments the following parameters were used. Flow rate: 0.8 ml/h, Voltage: 16 kV, Tip-to-collector distance: 15 cm.

Silver particles were produced at different concentrations of ethanol, water, silver nitrate, reducer, polymer, and surfactant. The completion of reduction was tested by XRD. The reduced product was separated by centrifugation and dried at 60 °C. Then, XRD pattern was obtained by an X-Ray Diffractometer (RIGAKU D/Max-2200/PC) using CuKα ($\lambda = 0.154$ nm) radiation at 40 kV and 200 mA). Furthermore, the distribution of silver nanoparticles in/on electrospun fibers was analyzed by SEM. The effect of rate of addition of hydrazine hydrate on reduction rate was also studied.

For SEM (Zeiss Evo 50) characterization, samples were placed on carbon tape and coated with carbon. In order to differentiate metal and the polymer effectively, electron back scattering probe was used.

2.2. Oleylamine/Oleic Acid System

In this system, metal nanoparticles were synthesized in hexane, and it is used as core solution in coaxial electrospinning. The shell solution is prepared separately.

In order to synthesize metal nanoparticles, silver ions were reduced and capped by oleylamine (Sigma Aldrich, 70%) and oleic acid (Riedel-de-Haën, technical grade) in *n*-hexane (Merck, ≥95%) which is used as solvent. First, silver nitrate which is the precursor for silver ions was dispersed in the solution of oleylamine and hexane through sonication. Then, oleic acid was added into the solution and mixed at high temperatures. After the accomplishment of the reaction, the solution was cooled down to room temperature. In order to understand the reaction dynamics, the effect of temperature, reaction time, and mixing condition were investigated in addition to the concentration effects of oleylamine, oleic acid, and hexane. The particle size and the size distribution of produced silver nanoparticles were determined to evaluate the effects of these parameters.

The structure of silver and silver compounds in the system was estimated by using XRD. Additionally, the size of the particles were estimated from the Scherrer equation (Eq. (1)) by using full width at half maximum value (FWHM), which is estimated by deconvolution of XRD patterns. The patterns were deconvoluted using Peak Fit software (Peakfit, v.4.11).

$$\langle L \rangle s_{\text{vol}} = \frac{k\lambda}{B_{1/2} \cos \theta_B} \quad (1)$$

In this equation, $\langle L \rangle s_{\text{vol}}$ is the volume weighted size, θ_B is the Bragg angle, λ is the wavelength of the X-ray, K is a unit cell geometry dependent constant whose value for silver particles is given as 0.89 in the literature,[13] and $B_{1/2}$ is FWHM of the peak after correcting for peak broadening which is caused by the diffractometer. $B_{1/2}$ can be calculated from,

$$B_{1/2}^2 = B_{\text{obs}}^2 - B_{\text{m}}^2 \quad (2)$$

where B_{obs} is the measured peak width and B_{m} is the peak broadening due to the machine. Peak broadening caused by the machine was calculated by the estimation of FWHM value of almost perfect crystalline structure.

To prepare samples for XRD, silver particles were separated from hexane, oleylamine, and oleic acid mixture as much as possible by washing them with ethanol

and by centrifugation. Samples were centrifuged twice at 10,000 rpm at 20 °C for 10 min.

An additional particle size measurement of produced nanoparticles was done by dynamic light scattering technique using particle size analyzer (Nanosizer ZS, Malvern Instruments Ltd.). Samples for this measurement were prepared by diluting the original solution ten times with hexane. The analysis was performed at 25 °C and the solution was kept in polystyrene cells during measurement. For each measurement six subsequent measurements were conducted and results were taken by using photon correlation spectroscopy (PCS) analysis software. The data taken in volume based particle size distribution were converted to cumulative undersize data, and evaluated as such.

The morphology, size, and distribution of particles were studied by using TEM (FEI, G2F30). Samples for this analysis were prepared by diluting the solution twenty times and drop casting onto the carbon coated copper grid with 250 mesh. Samples were dried under vacuum at room temperature before the analysis.

To calculate the average particle size and size distribution of the particles using the TEM micrographs, ImageJ software was used. These three analysis methods (XRD, PCS, and TEM) were compared in terms of their accuracy for the particle average size and size distribution determinations.

UV-Vis spectrum (Schimadzu, UV-2550) was used to characterize optical properties of metal nanoparticles. By this analysis, average particle size and size distribution were also obtained. Sample solutions were diluted in appropriate proportions with hexane. Quartz cells were used in the measurements, and readings were collected in the range of 200–800 nm.

Several sets of the solution were prepared for coaxial electrospinning. Some of the experiments were conducted with direct electrospinning of the optimized solution as core, and some are conducted with hexane evaporated to increase the silver concentration at core. In order to enhance the electrospinning capability, dilute polyvinyl pyrrolidone (PVP, Sigma Aldrich, molecular weight: 1,300,000) in N-N-dimethyl formamide (DMF, Merck, ≥99.8%) solution was added to the optimized solution. Hexane was evaporated as much as possible to eliminate the phase separation in the mixture of DMF-hexane and to increase the concentration of silver in the solution. In the shell part, PVP in DMF and polycaprolactone (PCL, Sigma Aldrich, molecular weight: 180,000) in triflouro ethanol (TFE, Merck, ≥99%) solutions were used due to their high electrospinning capabilities.

The setup of the coaxial electrospinning was same as the single jet electrospinning setup used in electrospinning of hydrazine hydrate system. The only difference was the spinneret consisting of two capillary tubes with one inside the other. A stainless steel capillary was used in this study with an exit orifice diameter of 1.1 and 2.5 mm for inner and outer capillaries, respectively. The inner capillary tube acted as an electrode and connected to a high voltage source. Two separate syringe pumps were used in order to adjust the flow rates of the inner and the outer solutions independently.

The morphological characterization of cable structures was done by using SEM (Quanto 200F—Fei Field Emission Gun) and TEM. The samples were placed on double sided carbon tapes and micrographs were taken without any coating. For TEM characterization, double grids were used.

3. RESULTS AND DISCUSSION

3.1. Hydrazine Hydrate System

In the hydrazine hydrate system, DSS was used to form micelle structures, and polymer shielded reverse micelle structures were used to prevent agglomeration of particles. With the addition of metal salt to this solution, unstable reverse micelles were formed in the system and with the addition of PVA which is a hydrophilic polymer, reverse micelle structures were shielded and suspended in the solution of water and ethanol. In the absence of ethanol, it was observed that the produced silver particles settled down. On the other hand, when excess amount of ethanol was added to the solution, PVA could not be dissolved. Then, the amount of ethanol in the solution was optimized according to the observations done. The reduction of silver ions to metallic silver by the hydrazine hydrate was supported by the XRD analysis as shown in Figure 3.

For the optimization of the concentrations of other ingredients in the system, SEM micrographs of nanofibers were analyzed to see the formation of fiber structures and distribution of silver particles in these fibers. Furthermore, the addition rate of hydrazine hydrate solution to the system was also studied to see the effect of the decrease of the reduction rate. Figure 4 shows the SEM micrographs of typical unsuccessful sample and the sample after optimizations.

Before optimization, silver particles were observed to be heterogeneously distributed in/on the polymer matrix.

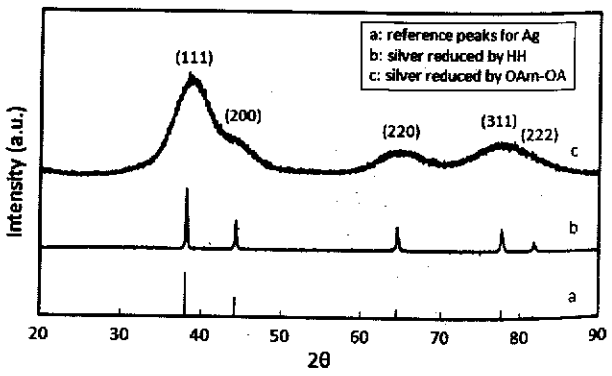

Fig. 3. XRD of silver obtained by using HH and OAm/OA.

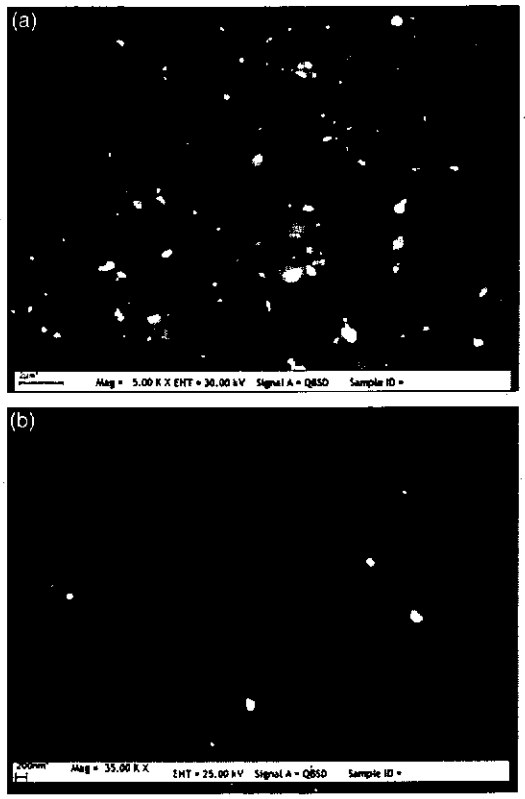

Fig. 4. SEM micrographs of two typical fibers produced by using hydrazine hydrate, (a) before optimization, and (b) after optimization. (a: 0.104 M $AgNO_3$; 1.28 M DSS; $n_{EtOH}/n_{DIW} = 0.35$; $n_{HH}/n_{Ag+} = 2.5$; HH addition rate: 0.15 ml/h; b: 0.078 M $AgNO_3$; 1.28 M DSS; $n_{EtOH}/n_{DIW} = 0.35$; $n_{HH}/n_{Ag+} = 3.5$; HH addition rate: 0.15 ml/h).

The agglomeration of particles was observed. After all the improvements done in the system, although particles were placed into fibers and distribution of the particles was improved, agglomeration could be prevented to a satisfactory low limit in the micelle phase, and the assembly of reverse micelle structures could not be well obtained. During the parametric study, it was observed that the only parameters associated with the reduction reaction such as feed rate of hydrazine hydrate and the concentration of hydrazine hydrate resulted in significant changes in nanofibers implying that reduction step lead to the problems. Since hydrazine hydrate reduces silver ions harshly, capping agents or the other molecules cannot surround many silver particles in a short time. Due to their high surface energy, free particles form agglomerates to reduce the surface free energy. No matter which capping agent is used or which operational parameters are changed, agglomeration of particles cannot be effectively prevented and broad particle size distribution is obtained. Therefore, it is necessary to use strong capping agents with weak reducing agents in order to control the particle size and the size distribution. To demonstrate the feasibility of such a system, oleylamine/oleic acid system was studied in which both components act as reducing and capping agents at the same time.

3.2. Oleylamine/Oleic Acid System

The reaction kinetics could be well controlled by using strong capping agents and weak reducing agents. Oleylamine and oleic acid have aliphatic tails of 18 carbons, and with amine, and carboxyl acid functional groups, respectively. These functional groups attack the metal ions and form micelle. The aliphatic tail helps to keep micelles up in suspension in aliphatic solvents. Functional groups, on the other hand, act as reducing agents and reduce the metal ions inside the micelle. In this way, particle formation can be controlled somehow.

The nanoparticles obtained from the oleylamine/oleic acid system were analyzed by XRD to characterize the structures formed. The four peaks in Figure 3(c) indicate that silver particles having face-centered cubic crystal structure formed after reduction. Moreover, the extreme broadening in the peaks indicates that crystallites begin to lose their expected shape and imperfections increase with decrease in size. The occurrence of broadening in each plane and the proportionality in diffraction intensities mean that particle size decreased in each plane of crystallite and particles with spherical shapes formed.

In addition to the information obtained from the XRD pattern, TEM and PCS analysis were performed for further characterization of the nanoparticles formed. In order to obtain some correlation between these methods, three samples prepared in different conditions were analyzed in detail, and the other samples were characterized by PCS method in the light of the existing correlation. The TEM micrographs of these three samples are given in Figure 5. According to these micrographs, although particles were not in solution conditions while taking these micrographs, no agglomeration between particles was detected.

The average particle size and size distribution determined from each method were listed in Table I for comparison.

According to these results, particle size data obtained from TEM and PCS techniques are in good agreement with each other, whereas the one obtained from XRD data were slightly smaller than the other two. If the TEM micrographs are analyzed at higher magnifications (Fig. 5(b)), two different phases are observed.

It was known from the literature[14] that the length of the oleylamine sections between two nanowires was measured as about 1–2 nm. This implies the possibility of the existence of oleylamine/oleic acid molecules attached to the surface. However, the distinct layer may also be due to an entirely different reason; the less regularly arranged surface atoms may also cause such an appearance in TEM due to incoherent scattering.

The particle size determined from the peak broadening in the XRD pattern gives the size information from the coherently scattering part of the crystallites.

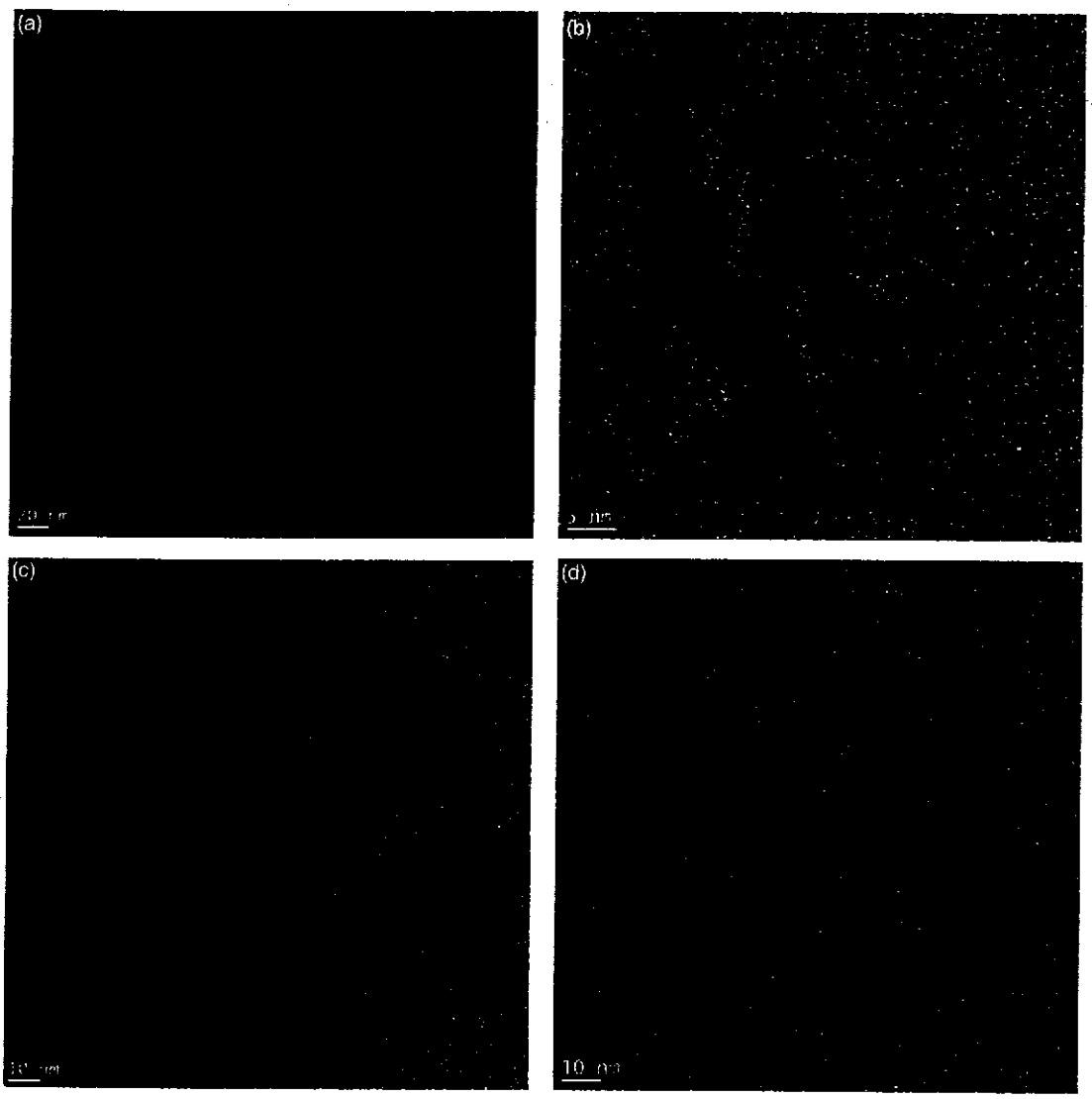

Fig. 5. TEM micrographs of (a) typical solution of metal nanoparticles, (b) at 115 °C, (c) at 150 °C, and (d) sonificated but magnetic stirring was not used.

The type of mixing, the reaction time and temperature, the concentrations of oleylamine, oleic acid, and silver nitrate also have large effects on silver particles produced. Mixing affects the particle size distribution, and it is shown in Figure 6.

When the solution was not mixed (Fig. 6(a)) two apparent phases occurred in the system indicating the incomplete reduction, and some of the silver ions remained in the solution. Besides the distribution has a tail at sizes below 2 nm. Figure 6(c) shows the particle size distribution when sonication was used only. The distribution is very uniform between 2–5 nm. In Figure 6(b) mechanical mixing is also involved besides sonication. It is seen that the distribution is uniform, and even finer than that in Figure 6(c).

Table I. Particle sizes calculated from different characterization methods.

Sample	TEM (nm)	PCS (nm) (volume-weight ave.)	XRD (nm) (Sherrer eq.n)
115 °C	2.8 ± 1.9	2.7	1.5
150 °C	3.8 ± 1.3	4.0	1.7
Sonication, but no mixing	2.8 ± 1.3	3.0	2.0

Time is another parameter that has significant effect on the properties of particles. The color of the solution during reaction changed from yellow to brown after one hour, and then, turned into dark brown after 1.5 hours. This color change indicated the completion of reaction according to the XRD and the PCS results. As seen in Figure 7, after a certain time, particle size distribution became broader due to particle growth. Then, the reaction time was fixed to be 2 hours for the experiments.

The increase of reaction temperature increases the particle size as seen from Table I, and it is also expected that the size distribution broadens with the increase of

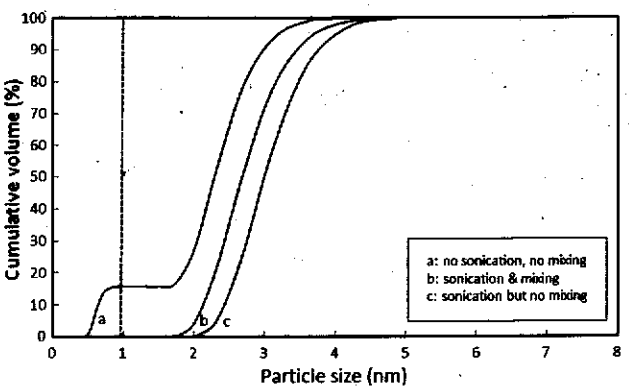

Fig. 6. Effect of mixing.

temperature as particles would adhere on each other. In fact no significant silver particles were produced below 115 °C. Weak reducing agents need higher temperatures than strong agents do for reduction reaction. Nevertheless, this provides an advantage to control the particle size by tuning the temperature.

In the absence of hexane, silver nitrate cannot be dissolved or dispersed in oleylamine. In the absence of oleylamine, it can be dispersed to a limited extent by sonication in hexane. When silver nitrate was mixed with oleylamine and hexane and then sonicated, a homogeneous dispersion was obtained. Capping of silver ions by oleylamine enhances further solubility of silver nitrate molecules. Oleic acid has a critical effect on the reduction mechanism of silver ions. In its absence the color of the solution stays yellow and does not turn into dark brown which is the indication of formation of metallic silver particles. For the concentrations of oleic acid less than a critical value, particles with size below 1 nm was observed in the PCS analysis, indicating an incomplete reduction. The incomplete reduction can be followed from Figure 8 given and discussed below. Furthermore, the small or insufficient amount of oleic acid results in the formation of larger particles. Actually, oleic acid enhances the dissociation of silver nitrate into silver and nitrate ions due to the interaction between carboxyl group of oleic acid and silver. Then,

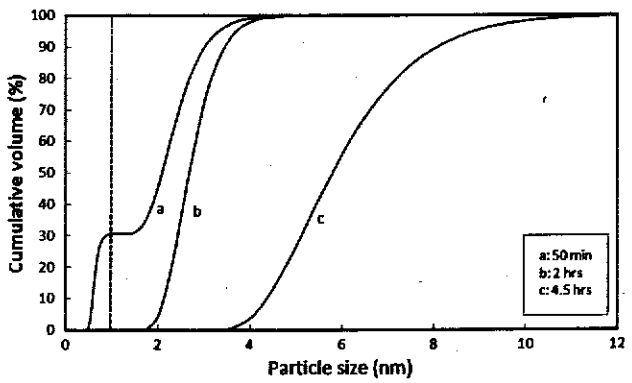

Fig. 7. Effect of reaction time.

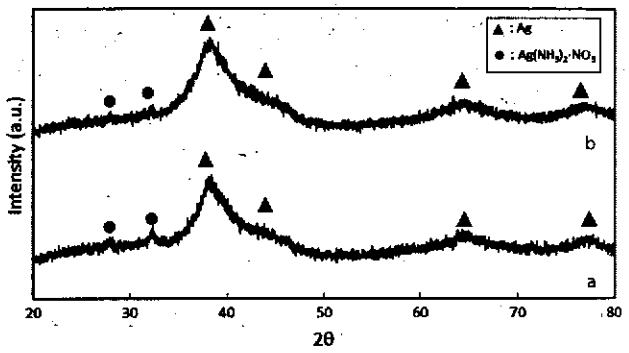

Fig. 8. XRD patterns of (a) sample with a reaction time of 50 min, and (b) sample where only sonication was done.

the silver ions are easily picked up by amine groups of oleylamine, and then reduced. Therefore as the amount of oleic acid increases there will be many micelles formed between silver ions and oleic acid-oleylamine, resulting in small size particles, otherwise large particles form. It can also be said in another way that as the amount of silver nitrate increases the particle sizes increase, and a broader distribution is obtained. Therefore, it is obvious that the dispersion of particles can be tuned by adjusting the concentrations of the components in the system.

It can be summarized that amine groups of oleylamine attract and encapsulate silver ions and thus enhance the dissolution of silver nitrate in hexane. Oleic acid added to the solution removes nitrate ions from silver by forming silver oleate. Then reduction reactions take place as given below. The complex formed between ammonia and silver reduces the reduction potential.

$$RCOOH + AgNO_3 \rightarrow RCOO^-Ag^+ + HNO_3 \quad (3)$$

$$Ag^+ + e^- \rightarrow Ag \qquad E^\circ_{red} = 0.799\ V \quad (4)$$

$$Ag(NH_3)_2^+ + e^- \rightarrow Ag + 2NH_3 \qquad E^\circ_{red} = 0.373\ V \quad (5)$$

The complexation of silver with ammonia slows down the reduction mechanism and makes easy to control the particle size distribution. The complex formation was demonstrated by XRD results for the samples in which the reaction was not yet completed. Figure 8 shows the XRD spectrum of the sample with a reaction time of 50 minutes. Both metallic silver and $Ag(NH_3)_2NO_3$ are detected at the proper 2θ values. Whenever peaks that belong to $Ag(NH_3)_2NO_3$ were observed in the XRD patterns, a second peak in the PCS plot always appeared below 1 nm (as can be seen in Figs. 6 and 7, curve a), leading to the conclusion that incomplete reduction can be traced indirectly from the front tail of the distribution.

SPR analysis was conducted to characterize the optical properties of silver particles. Figure 9 shows the UV-Vis spectrum of the samples prepared at 115 °C and 150 °C using the same concentrations.

The expected SPR absorption peak for silver is between 400–450 nm as reported in the literature.[15] The peak

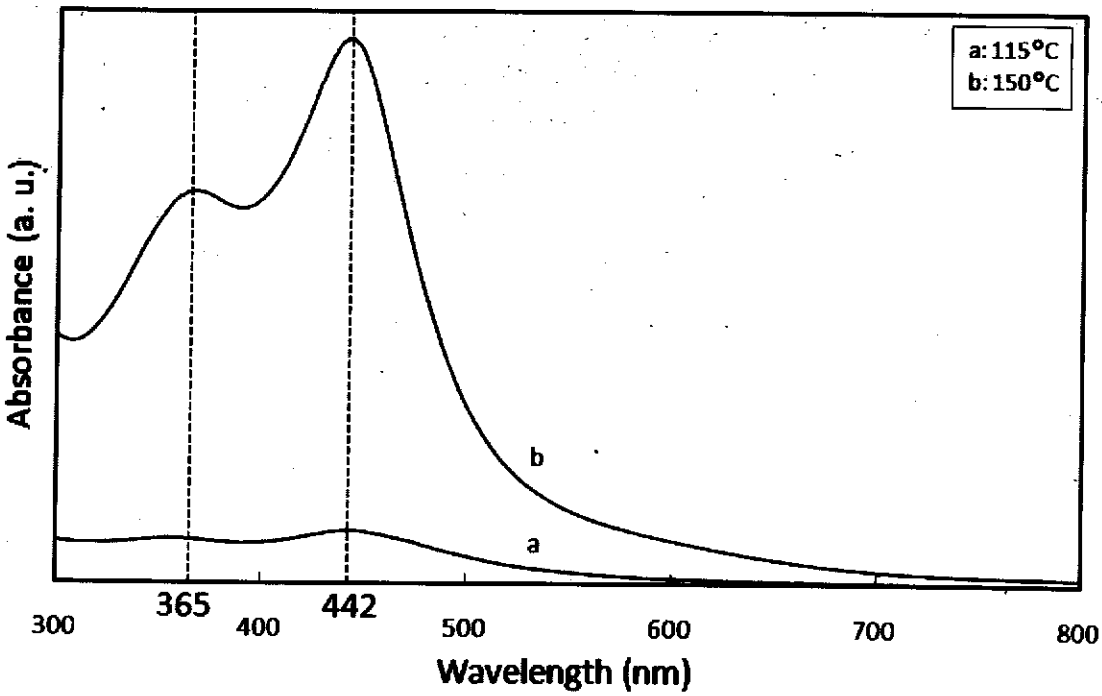

Fig. 9. UV-vis spectra of samples prepared at different reaction temperatures with 12.5 fold dilution; (a) 115 °C, and (b) 150 °C.

belonging to lower wavelength is generally attributed to particles with morphological differences.[15] The increase of the absorption intensity (i.e., peak heights) with temperature indicates that the particle size increases with temperature. This was also proved to be so by PCS and XRD analysis as seen from Table I.

After many trials an optimum procedure was developed as follows for the nanocable production step. For the solution, 2 mmol silver nitrate is dissolved in 20 ml oleylamine and hexane solution (50:50, v:v) by sonication; then, 6 mmol oleic acid is added into the solution and temperature is increased to 115 °C, and mixed by a magnetic stirrer for 2 hours. Figure 10 shows the size distribution of particles to be used in the following steps. The average size of these particles was found to be 2.7 nm.

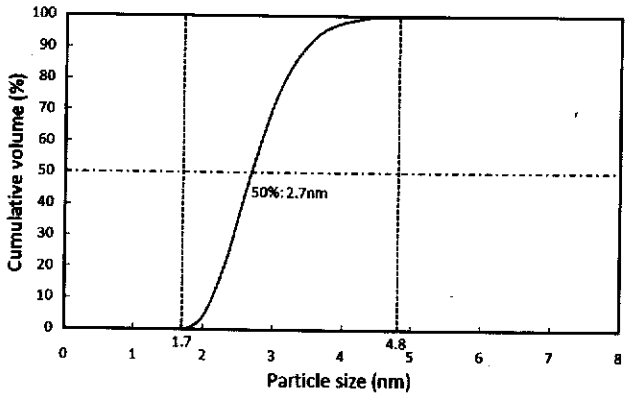

Fig. 10. Size distribution of particles of the optimized solution.

3.3. Nanocable Production

The above mentioned optimized solution silver nanoparticles were used as core solution for nanocable production by electrospinning. As polymer solutions PVP in DMF, and PCL in TFE were used. The parameters of the system were adjusted according to the observations of the Taylor cone formed at the coaxial capillary tip. When PVP in DMF was used as the shell solution silver particles deposited on fibers, and they were not connected with each other (Fig. 11).

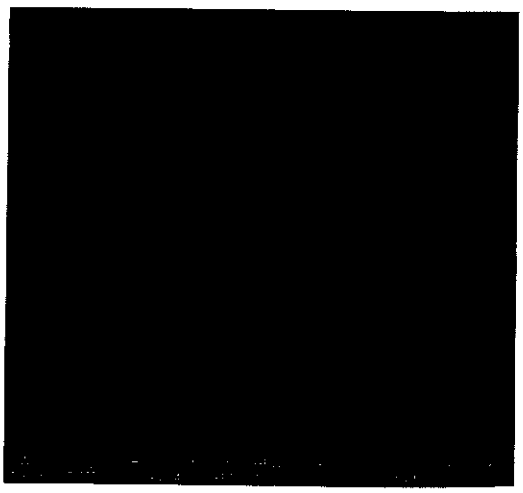

Fig. 11. SEM micrograph of the fibers (shell: 20 wt% PVP in DMF solution; flow rates, inner: 0.1 ml/h, outer: 0.4 ml/h; tip-to-collector distance: 14 cm; voltage: 15 kV).

The aggregation of silver nanoparticles could be accomplished if they were concentrated. This was achieved by evaporating hexane as much as possible; it in turn yielded a concentrated solution. It improved the situation, but still the particles are well below percolation threshold as seen from Figure 12.

PVP in DMF is a good but not the best polymer solution for the electrospinning of such a system and it was difficult to adjust parameters of electrospinning. For instance, when the flow rate of the core solution increased the flow rate of the shell solution should also increase accordingly to carry the inner solution carrying the metal. However, it turned out that fibers became too thick; and either Taylor cone could not easily form or it was not stable. Finally, fibers could not be well produced or dried. To overcome this difficulty, the concentration of PVP in DMF solution was increased to 30 wt% to increase its carrying capability. However, this solution was extremely viscous to electrospin. An improvement was attempted by substituting DMF with deionized water due to its lower boiling point; and it did not work either. Then the shell solution was changed, and PCL in TFE was used. It is easy to electrospin it due to the high polarity of polymer and solvent. As shell solution 8 wt% PCL in TFE was used. Figure 13 shows the micrograph of this sample, and it is seen that there has been highly satisfactory improvement. The silver nanoparticles could be observed like continuous wires at the center.

To achieve further improvement hexane was evaporated to concentrate silver particles. Then there has been outstanding improvement; and the silver particles aligned in the core to form continuous nanowire inside the PCL sheath as seen from Figure 14. Cable structures appear in all fibers in the micrograph.

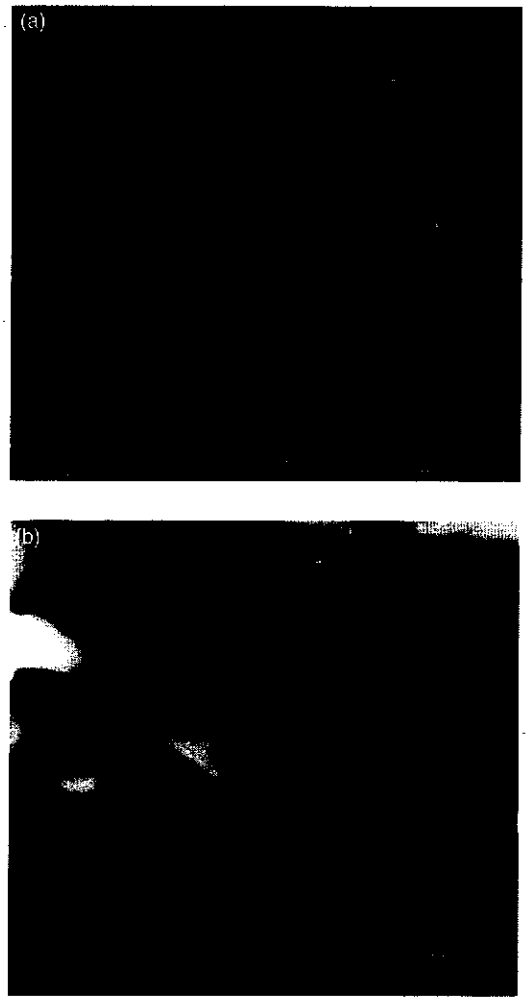

Fig. 13. SEM micrograph of the fibers (shell: 8 wt% PCL in TFE solution; (a): flow rates, inner: 0.1 ml/h, outer: 0.4 ml/h; tip-to-collector distance: 14 cm; voltage: 15 kV; and (b) flow rates, inner: 0.3 ml/h, outer: 1 ml/h; tip-to-collector distance: 20 cm; voltage: 20 kV).

Fig. 12. SEM micrograph of the fibers (core: optimized solution with hexane evaporated, shell: 20 wt% PVP in DMF solution; flow rates, inner: 0.4 ml/h, outer: 2 ml/h; tip-to-collector distance: 14 cm; voltage: 17 kV).

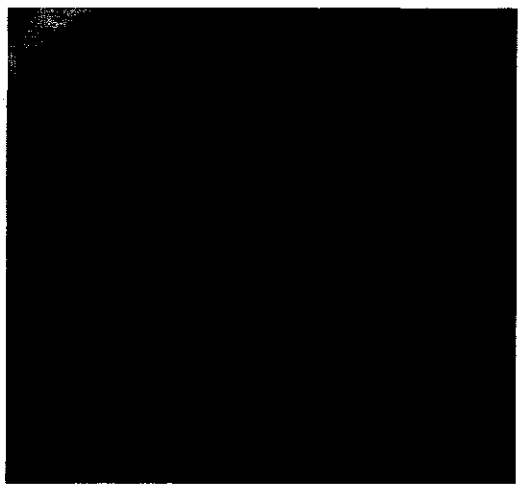

Fig. 14. SEM micrographs of the fibers when hexane was evaporated (shell: 8 wt% PCL in TFE solution; flow rate, inner: 0.4 ml/h, outer: 1 ml/h; tip-to-collector distance: 18 cm; voltage: 16 kV).

Fig. 15. SEM micrograph of the fibers with 5 wt% PVP in DMF added to the core solution (flow rate, inner: 0.1 ml/h, outer: 1.5 ml/h; tip-to-collector distance: 16 cm; voltage: 17 kV).

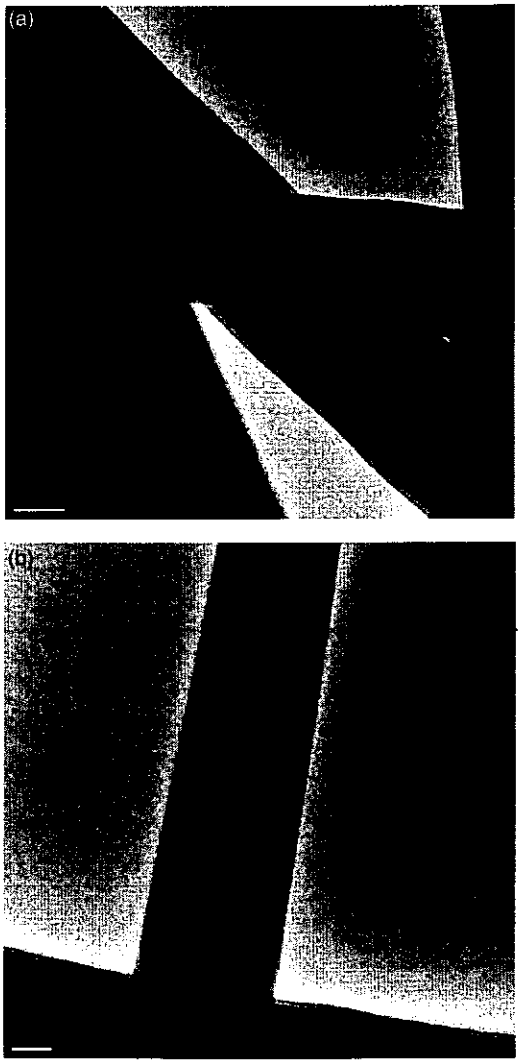

Fig. 16. TEM micrograph of cables.

A final improvement was realized for the core solution for PCL in DMF system. In order to improve the compatibility between the core and the shell solutions small amount of PVP in DMF solution (5 wt%), was added into the core solution. Since hexane and DMF do not dissolve in each other, hexane evaporates from the solution. The produced fibers of this sample were also in cable structure but some relatively thicker fibers formed as seen from Figure 15.

The cable structures were further examined by using TEM. It is seen from Figure 16 that silver nanoparticles formed a continuous wire at the center.

4. CONCLUSION

In this study, it was shown that it is very difficult to control size and size distribution of particles below 20–30 nm with strong reducing agents like hydrazine hydrate. Oleylamine/oleic acid system on the other hand, is simple and versatile to produce monodispersed metal nanoparticles with controlled sizes below 10 nm due to the strong capping and slow reduction characteristics of the mixture. Oleylamine and oleic acid enhance the dissolution of silver nitrate in hexane. Since silver ions form complex with oleylamine and oleic acid the reduction mechanism slows down, and the size of nanoparticles can be controlled. Silver nanoparticles with sizes between 1.7 nm and 4.8 nm and volume-weighted average of 2.7 nm were produced through oleylamine/oleic acid system. The synthesized metal nanoparticles were properly aligned in the core of the continuous polymeric fibers produced by coaxial electrospinning. PVP forms a good sheath for the silver nanowire at the center.

Acknowledgment: This research was supported mostly by TÜBİTAK (Turkish Scientific and Research Council) under Grant No. MAG-107M024, and also by ODTÜ-BAP-2006-07-02-00-01.

References and Notes

1. C. S. S. R. Kumar, Nanomaterials for the Life Sciences, edited by C. S. S. R. Kumar, Wiley-VCH, Weinheim, Germany **(2009)** Vol. 1, p. 571.
2. T. Song, Y. Zhang, T. Zhou, C. T. Lim, B. Liu, and S. Ramakrishna, *Chem. Phys. Lett.* 415, 317 **(2005)**.
3. T. M. Tolaymat, A. M. El Badawy, A. Genaidy, K. Schekel, G. Luxton, and M. Suidan, *Sci. Total Environ.* 408, 999 **(2010)**.
4. G. S. D. Dinabandhu, *Metall. Mater. Trans. B* 39 B, 35 **(2008)**.
5. M. A. S. Sadjadi, B. Sadeghi, M. Meskinfam, K. Zare, and J. Azizian, *Physica E* 40, 3183 **(2008)**.
6. Y. Ho, Z. Xu, and S. Sun, *Angew. Chem. Int. Ed.* 46, 6329 **(2007)**.
7. Z. Xu, C. Shen, Y. Hou, H. Gao, and S. Sun, *Chem. Mater.* 21, 1778 **(2009)**.
8. V. Mazumder and S. Sun, *J. Am. Chem. Soc.* 131, 4588 **(2009)**.
9. I. C. Chiang and D. H. Chen, *Nanotechnology* 20, 015602 **(2009)**.

10. P. de la Presa, M. Multigner, J. de la Venta, M. A. Garcia, and M. L. Ruiz-Gonzalez, *J. Appl. Phys.* 100, 123915 (**2006**).
11. M. Klokkenburg, J. Hilhorst, and B. H. Erné, *Vib. Spectrosc.* 43, 243 (**2007**).
12. C. Wang, Y. Hu, C. M. Lieber, and S. Sun, *J. Am. Chem. Soc.* 130, 8902 (**2008**).
13. Z. Deng, M. Mansuipur, and A. J. Muscat, *J. Phys. Chem. C* 113, 867 (**2008**).
14. X. Lu, M. S. Yavuz, H. Y. Tuan, B. A. Korgel, and Y. Xia, *J. Am. Chem. Soc.* 130, 8900 (**2008**).
15. B. Wiley, Y. Sun, B. Mayers, and Y. Xia, *Chem. Eur. J.* 11, 454 (**2005**).

Received: 11 June 2010. Accepted: 29 July 2010.